HIGH-POWER SWITCHING BY MULTI-GRID IGNITRONS

By
T. F. Turner
and
H. S. Butler

Internal Memorandum
M Report No. 257
March 1961

PROJECT M
STANFORD UNIVERSITY
STANFORD, CALIFORNIA

HIGH-POWER SWITCHING BY MULTI-GRID IGNITRONS

By

T. F. Turner

and

H. S. Butler

Internal Memorandum
M Report No. 257
March 1961

Project M
Stanford University
Stanford, California

SUMMARY

This report describes an investigation which had as its major purpose the development of a high-power switch for use in the modulators for the proposed Stanford two-mile linear electron accelerator. It has been found that existing ignitron tubes can be used to switch current pulses of thousands of amperes and several microseconds duration at repetition frequencies of hundreds per second while holding off voltages of tens of kilovolts. The performance of a typical switch is described in detail with regard to: (1) maximum reliable hold-off voltage, (2) maximum peak current capability, (3) maximum peak power capability, (4) average power capability, (5) pulse-time jitter and anode delay, and (6) effective deionization time.

Several additional experimental observations are reported here which provide some insight into the pulsed operation of the ignitron and which were used as guideposts in the design of an ignitron specifically for high-power switching purposes.

A complete schematic for an 87 Mw, 110 kw modulator is also included.

TABLE OF CONTENTS

LIST OF FIGURES

I. INTRODUCTION

Since the Spring of 1959 an effort has been made to find a device to serve as the high-power switch for use in the modulators for the proposed Stanford two-mile linear electron accelerator.[1] Briefly, the switch had to make possible the development of modulators having the following principal specifications:

Peak power output (max)	64 Mw
Average power output (max)	74 kw
Output pulse voltage range	158-248 kv
Output pulse current range	120-258 amps
Load impedance range	1320-962 ohms
Pulse length (flat-top)	2.50 μsec
Rise and fall times (max 0-100%)	0.7 μsec
Pulse repetition rate	60, 120...360/sec
Pulse height deviation from flatness (max)	± 0.5%
Pulse time jitter (max)	± 10 mμsec
Pulse-to-pulse amplitude jitter (max)	± 0.25%

In addition, the modulator had to be the design that would be most economical when maintenance and operating costs over a ten-year period were taken into account.

The first part of the switch investigation led to the conclusion that the spark-gap devices and hydrogen thyratrons then in existence or under development were not capable of meeting all of the switch requirements. We therefore undertook, more or less as a last hope, an investigation of the performance of ignitrons as high-power switches.

---

1. All references appear at the end of the text.

II. DESCRIPTION OF IGNITRONS

For the most part, the ignitron tubes tested at Stanford have been of the multi-grid sealed-off design. Although the literature contains several descriptions of ignitrons,[2,3] a brief review of the tube structure and processing is given here for convenience. Figures 1 through 4 illustrate the internal structure of several specific designs.

The conventional ignitron consists of a sealed envelope containing a mercury-pool cathode, one or more ignitors, an anode, and one or more grids used for various purposes. An important part of the tube is its external integral water jacket which allows reasonably close but not complete control of the internal mercury-vapor temperature and pressure. (It is known that under operating conditions the mercury-vapor pressure is somewhat higher than that associated with the water in the external jacket.) Auxiliary anodes near the mercury pool may be included in some cases.

The tubes discussed in this paper are processed much like high-vacuum tubes during manufacture, i.e., all but the glass seal is baked at a temperature of approximately 700°C for a period of about eight hours. While baking, the tubes are pumped with high-quality mercury diffusion pumps. After evacuation a metered amount of specially purified mercury is admitted and the tube is sealed off.

Typical ignitors are made of a refractory material. The material used varies from manufacturer to manufacturer, as does the processing of the material during manufacture. In general, the materials are mixed, extruded to cylindrical shape, and fired to a high temperature in a disposable graphite crucible under pressure. The completed ignitor rod

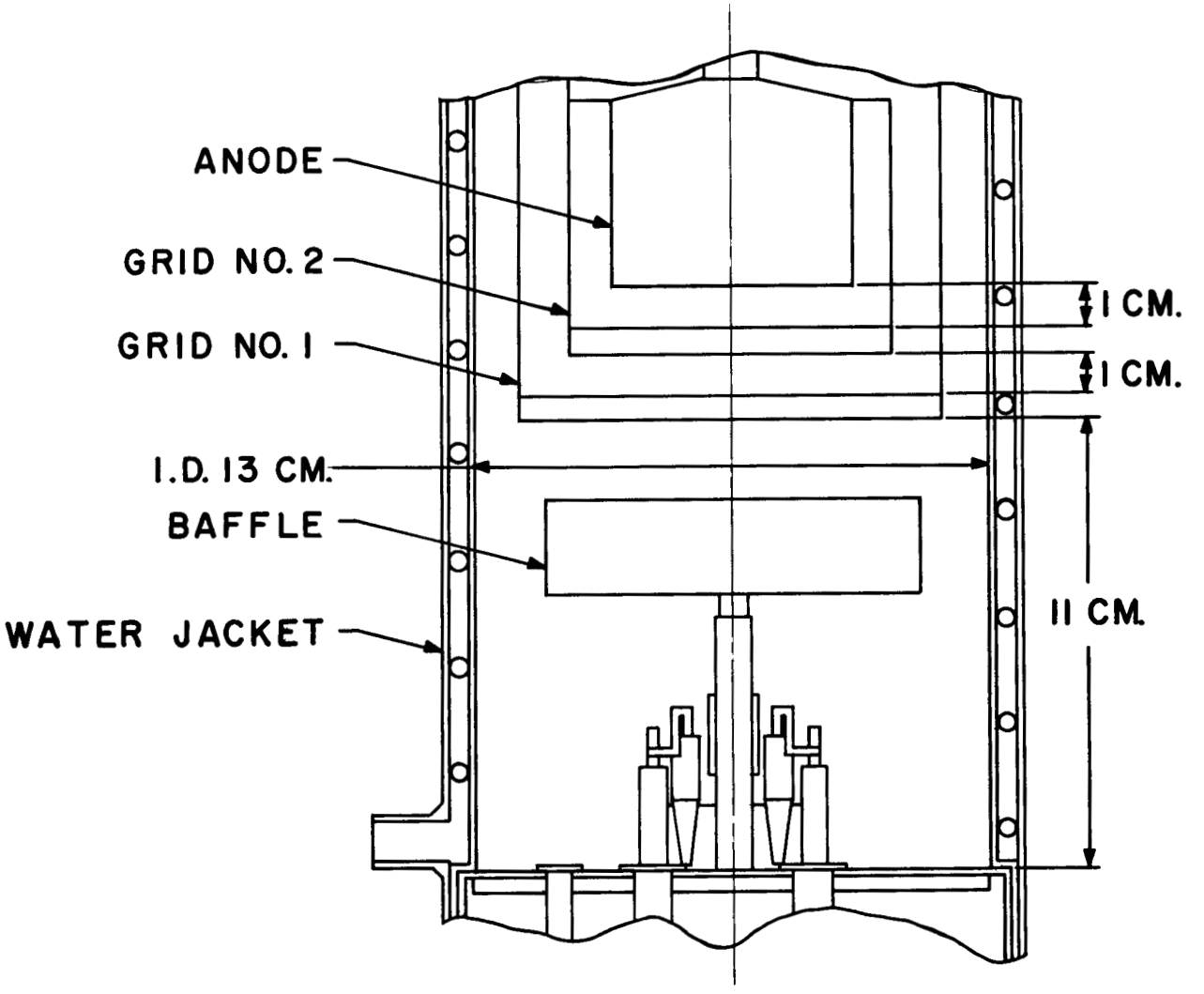

FIG. 1 INTERNAL STRUCTURE OF TYPE 5630 IGNITRON

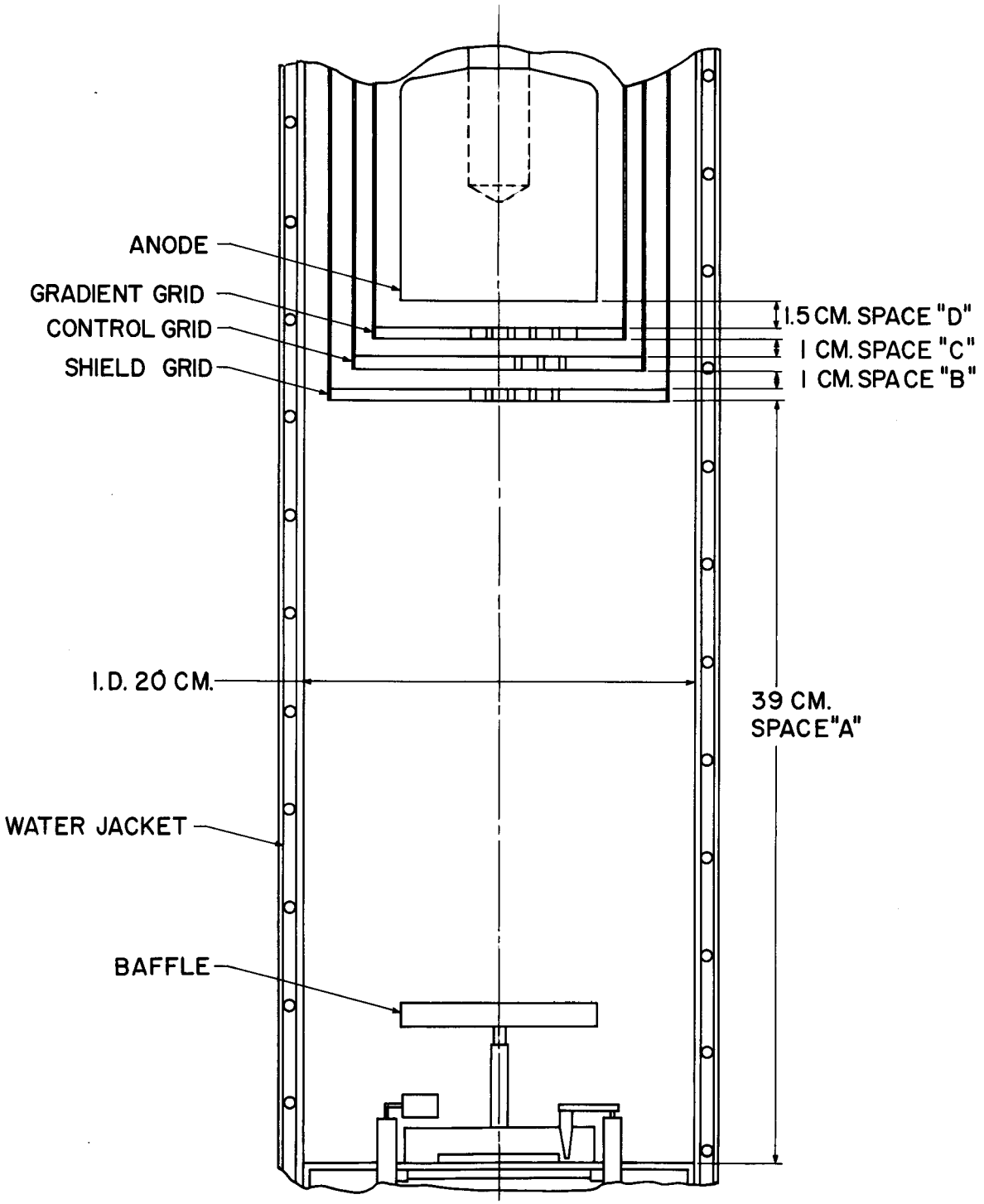

FIG. 2 INTERNAL STRUCTURE
OF TYPE 6228 IGNITRON

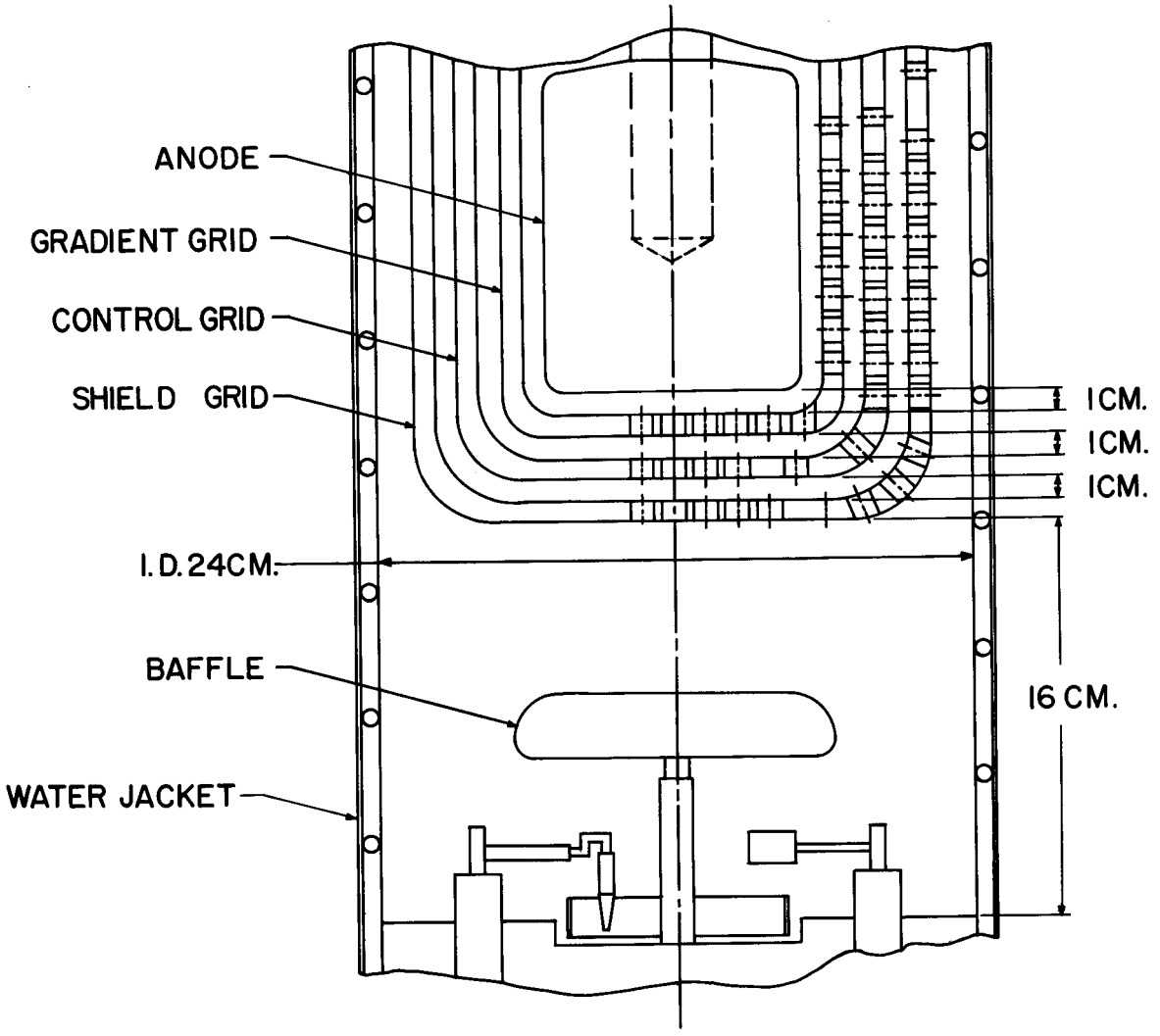

FIG.3 INTERNAL STRUCTURE
OF TYPE Z5233 IGNITRON

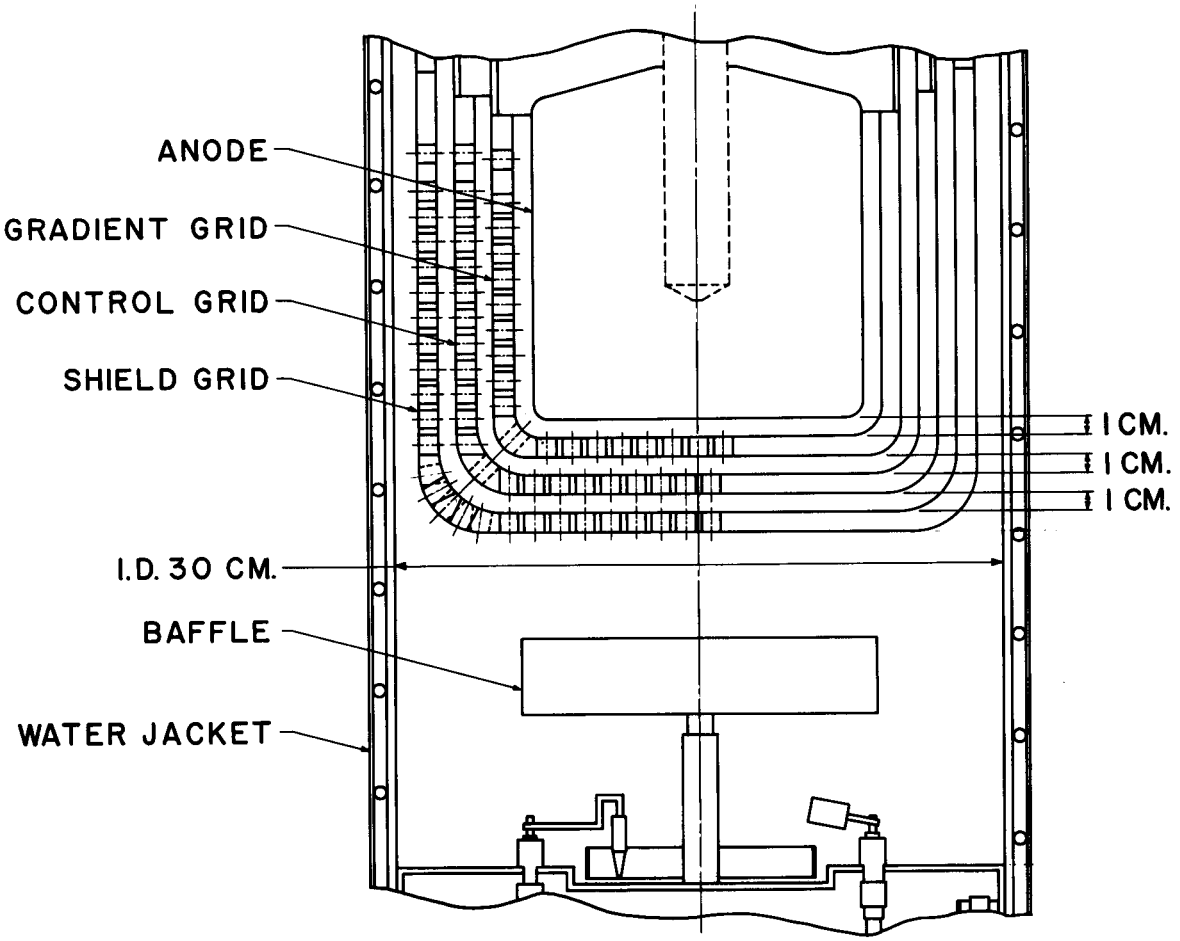

FIG. 4 INTERNAL STRUCTURE
OF TYPE Z5234 IGNITRON

is pointed by grinding and is mounted on a molybdenum or Kovar rod in assembly.

While the exact mechanism of cathode formation by ignitor firing is not known to the authors at this time, several observations can be made which may be helpful in tube application.

First, the ignitor appears as a nonlinear circuit element. This behavior is illustrated by the typical voltage and current curves shown in Fig. 5. In addition, it is an experimental fact that the ignitor appears to dc or a very slowly changing voltage as though it were a low resistance (of the order of 50-100 ohms) which itself is a slowly varying function of the applied dc voltage.

A photographic examination of ignitor operation by Cummings[4] has shown that the spot of cathode activity surrounding the ignitor propagates rapidly out over the surface of the cathode pool after breakdown. The velocity of propagation inferred by Cummings is about 2×10^5 to 2×10^6 cm/sec. (This value is dependent on total cathode current and must be regarded as approximate.) Therefore, by waiting a period of 2 microseconds after application of the ignitor pulse before the application of the grid pulse, there is reasonable assurance that the main pulse current discharge will come from the central region of the cathode pool and not from the ignitor stub itself, thus prolonging the life of the ignitor.

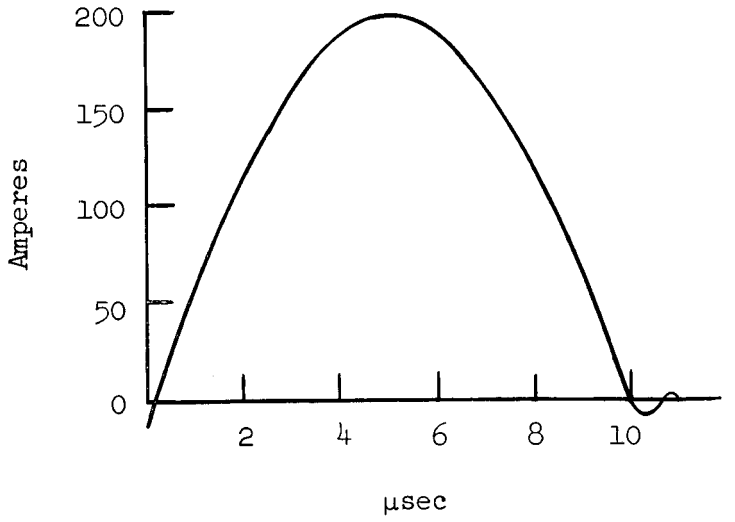

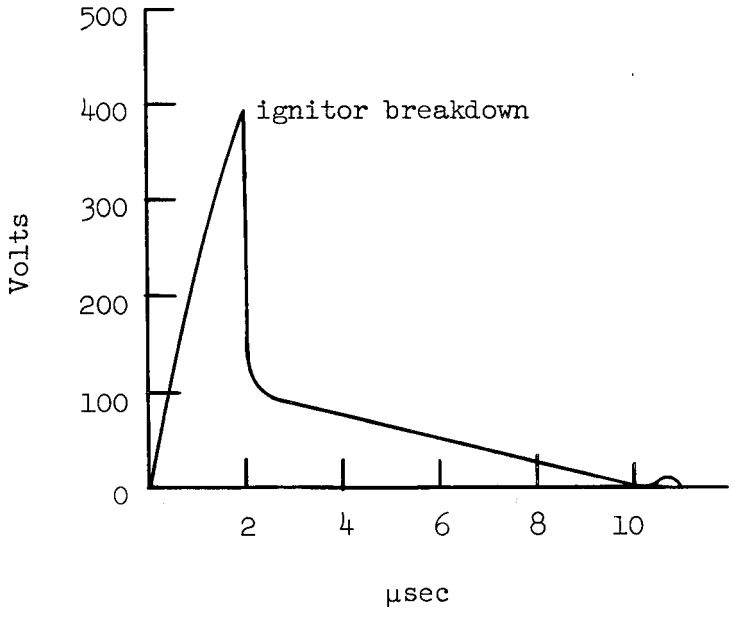

FIG. 5--Typical ignitor voltage and current characteristics.

III. TYPICAL SWITCH PERFORMANCE

To date, only two types of gridded ignitrons have been extensively tested in this laboratory, namely, the GL-6228 and Z5233. For our purposes, the GL-6228 performs more satisfactorily than the Z5233. Tests presently in progress on the type Z5234 have not shown any advantages over the GL-6228 for our work. The following discussion will therefore be confined to the performance of the GL-6228.

The GL-6228 has been tested in various circuit configurations to allow independent measurement of the following parameters:

1. Maximum reliable hold-off voltage
2. Maximum peak current capability
3. Maximum peak power capability
4. Average power capability
5. Pulse-time jitter and anode delay
6. Effective deionization time

These tests will be described in order and the results of each will be given below.

1. Maximum Reliable Hold-Off Voltage

The reliable hold-off voltage is a function of the water jacket temperature, the method of biasing the tube, and the average power dissipation. For the purposes of this paper, maximum hold-off voltage is defined as the highest anode voltage that can be applied for a period of 30 minutes without tube malfunction. The following table gives the results of this test for the GL-6228 with optimum bias.

Average Power	Outlet Water Temp.	V_{max}
$\leq$ 10 kw	$30 < t < 45^{\circ}C$	60 kv
~ 25 kw	$t = 45 \pm 1^{\circ}C$	60 kv*
55 kw	$t = 40^{\circ}C$	50 kv
75 kw	$t = 36^{\circ}C$	45 kv
110 kw	$t = 36^{\circ}C$	45 kv

*The data on line two were obtained independently by Craggs and Meek[6] at prf = 750 cps.

Here, average power = $1/2\ C_n\left(V_{max}\right)^2$ prf, where C_n is the network total capacity, V_{max} is the maximum hold-off voltage, and prf is the pulse repetition frequency. These measurements were made at various repetition frequencies at or below 360 pps.

2. Maximum Peak Current Capability

Tests to determine an absolute peak current capability in modulator service serve very little purpose. However, an attempt was made to find a reasonable upper limit by connecting the tube under test in a Blumlein circuit and running at optimum bias and optimum water temperature at a prf of 120 cps. At our full power-supply capability, under the above conditions, we observed stable operation as follows:

Pulse length = 3.7 microseconds

Peak current = 8600 amperes

Peak power = 144 Mw

Average power = 64 kw

V_{max} = 33.6 kv

These tests and much of the information gleaned from various applications of ignitrons in crowbar service[7] indicate that there is virtually no limit to cathode emission capability in ignitrons of this type.

3. Maximum Peak Power Capability

To date, 144 Mw is the maximum peak power switched with the GL-6228. As noted in the discussion of peak current capability, this value was limited by the rating of our power supply and should not be taken as an upper limit on the performance capability of the ignitron as a switch.

4. Average Power Capability

We have successfully operated the tube for a period of 48 hours at 110 kw average. Testing at high average power levels will continue as soon as practical circumstances make it possible; we have been able to operate for short periods of time (15-20 minutes) at average powers of 150 kw. The limiting factor in high average power testing has thus far been the auxiliary apparatus and not the switch tube.

5. Pulse Time Jitter and Anode Delay

Under optimum bias conditions, as discussed below, and at an average power of 64 kw, the pulse-time jitter has been shown to be less than 4.0 millimicroseconds. Measurement of jitter to high accuracy is a sophisticated circuit problem when these power levels are involved (because of cross-talk, etc.). Time has not permitted us to refine our measurement techniques to the point where it is possible to present more accurate information. Anode delay seems to be of the order of one-half microsecond and stable.

6. Effective Deionization Time

We are primarily interested in the maximum repetition frequency at which the tube can be operated, rather than the deionization time as such.

Because various regions of the mercury-vapor space within the tube take radically different times to deionize, it is difficult to define a specific deionization time. Suffice it to say here that without delayed charging circuitry the tube will operate satisfactorily at 110 kw average power at 360 pps. Craggs and Meek[8] report operating at 25 kw average and 750 pps. As of this writing we believe that operation at pulse repetition rates of 1000 or even 2000 per second would be possible at 75 kw average power, but we do not have the facilities to test this supposition.

IV. DISCUSSION OF PULSED IGNITRON OPERATION

During the course of this investigation a number of experimental observations were recorded which appear to have an important bearing on the theory of the pulsed operation of ignitrons. Since no quantitative theory dealing with the subject is known to the authors, it seems desirable to recount these findings in the hope that they will contribute to an increased understanding of ignitron operation.

A convenient way to discuss the pulsed operation of ignitrons is to divide the pulse cycle into three periods, which we shall discuss in the following order: (1) the hold-off period, (2) the post-pulse period, and (3) the pulse period. The hold-off period is of the order of milliseconds long; we shall consider the condition of the tube just before firing. The post-pulse period of interest is about two milliseconds. The pulse period, during which the pulse current is flowing, is of the order of a few (say three) microseconds. The way in which the events in any one of the periods affect behavior in the succeeding period will be discussed below.

1. Hold-Off Period

During the hold-off period the potential distribution within the tube must be such that no conduction can occur. Generally speaking, Paschen's law[9] is expected to dictate the correct voltage distribution, since it relates the potential that can exist perpendicular to a gap without breakdown to the gas pressure within the gap. Figure 6 shows the experimentally derived voltage distribution within the tube which was found to be the most satisfactory one for pulsed operation. Insofar as hold-off is concerned, the most critical space is that between the

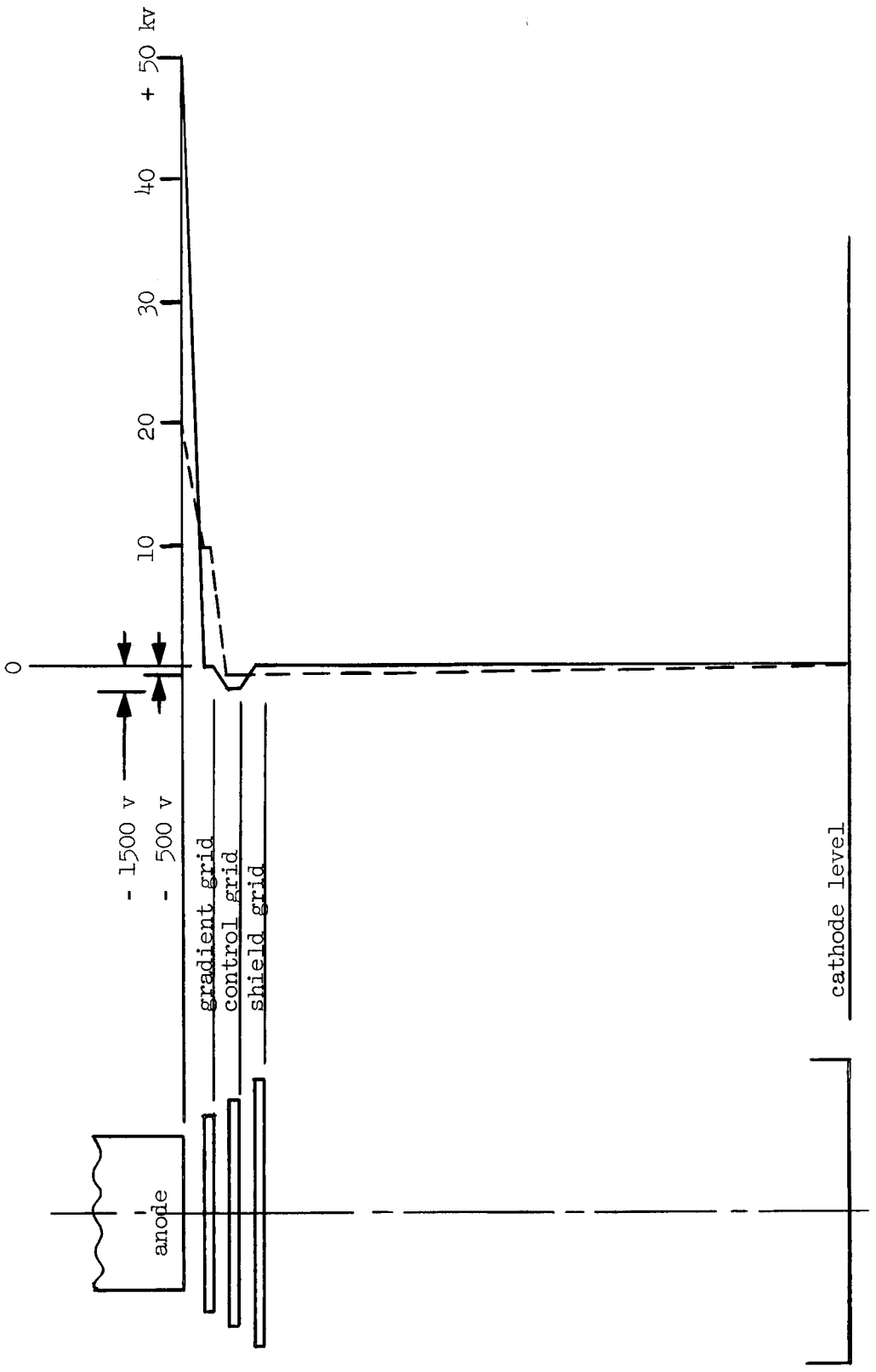

FIG. 6--Typical pulse service voltage distribution (solid line) compared to recommended rectifier service voltage distribution (dashed line) for tube type GL-6228.

anode and the gradient grid, across which 50 kv is dropped. Unfortunately no reliable Paschen's breakdown curve (sparking potential vs reduced electrode distance) is available for the range of reduced electrode distances pertinent to the GL-6228; experimental work in this range is quite difficult. Even if such a curve were available, it is almost impossible to assign a reliable value to the ion density in the anode-gradient grid region because the high operating temperature of the anode introduces a density gradient in this region whose effect is difficult to assess. Thus a correlation direct with Paschen's law is not possible at present, although this law did influence the direction of our experimentation. Nevertheless, two important points can be made. (1) When the ignitron is used in pulsed operation the voltage distribution must be altered from that associated with non-pulsed operation (e.g., high-potential testing) because the space between the mercury pool and the shield grid stays ionized, as will be discussed in the next section. For comparison purposes the recommended voltage distribution for the GL-6228 when used in conventional rectifier operation is included in Fig. 6. (2) The voltage distribution shown in Fig. 6 is the final result of an exhaustive program of experiments to derive the distribution that provided the most stable and reliable operation and that reduced the spurious currents inherent in the post-pulse period to a minimum. Variations from this distribution of only a few percent reduce the tube performance below its optimum.

2. Post-Pulse Period

This period will be considered next because it provides some insight into what occurs during the pulse period. Following the end of the

current pulse, it was found experimentally that the shield grid-cathode voltage drop remained constant for a time which may exceed two milliseconds at high peak currents. Curves typical of this performance are shown in Fig. 7. Note that the time corresponding to the break-point increases with increasing current. These curves have been interpreted in terms of residual ionization. The ions formed during the pulse period require a finite time to decay. This time will be referred to as the deionization time. The break-point on each curve implies that the ion density, created initially by the current pulse, has decayed to a certain minimum ion density below which full conduction cannot be supported. This minimum ion density is fixed by the tube geometry.

Figure 8a shows the deionization time in the shield grid-cathode region as a function of peak current for two different values of the cooling-water temperature. Figure 8b shows the analogous data for the region around the control grid. Note the much shorter deionization times associated with the control grid region. Since the volume-to-surface ratio is much smaller in this area than in the area between the cathode and the shield grid, the deionization time is correspondingly shorter, because the major deionization process is recombination at the wall. The most notable feature of these graphs is the fact that the deionization time approaches a maximum value. This implies that the ion density created initially by the current pulse approaches a maximum value and that this maximum value can only correspond to 100% ionization of the mercury vapor. Thus, the deionization time is intimately associated with the degree of ionization.

Two additional observations relating to the deionization time were made. As is apparent from Figs. 8a and 8b the deionization times in

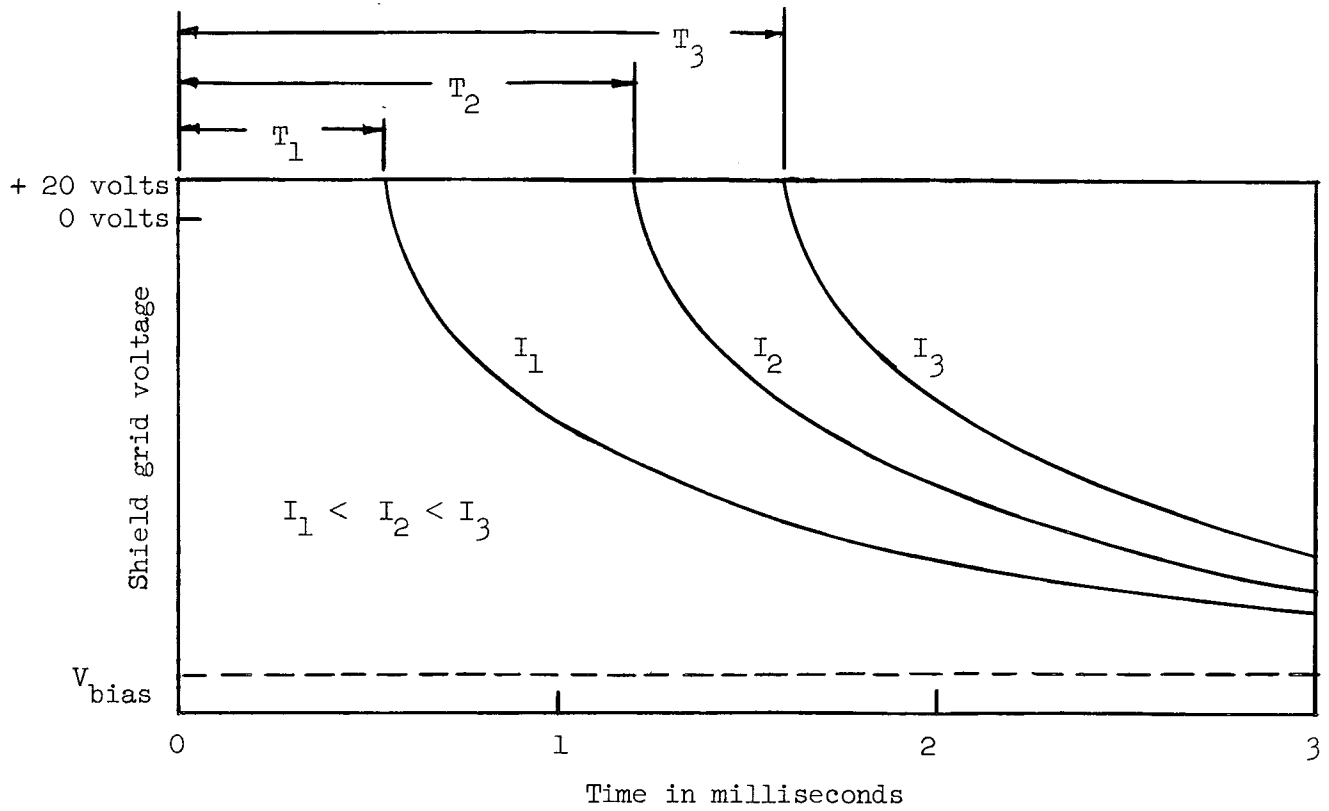

FIG. 7--Shield grid voltage as a function of time for three values of peak current.

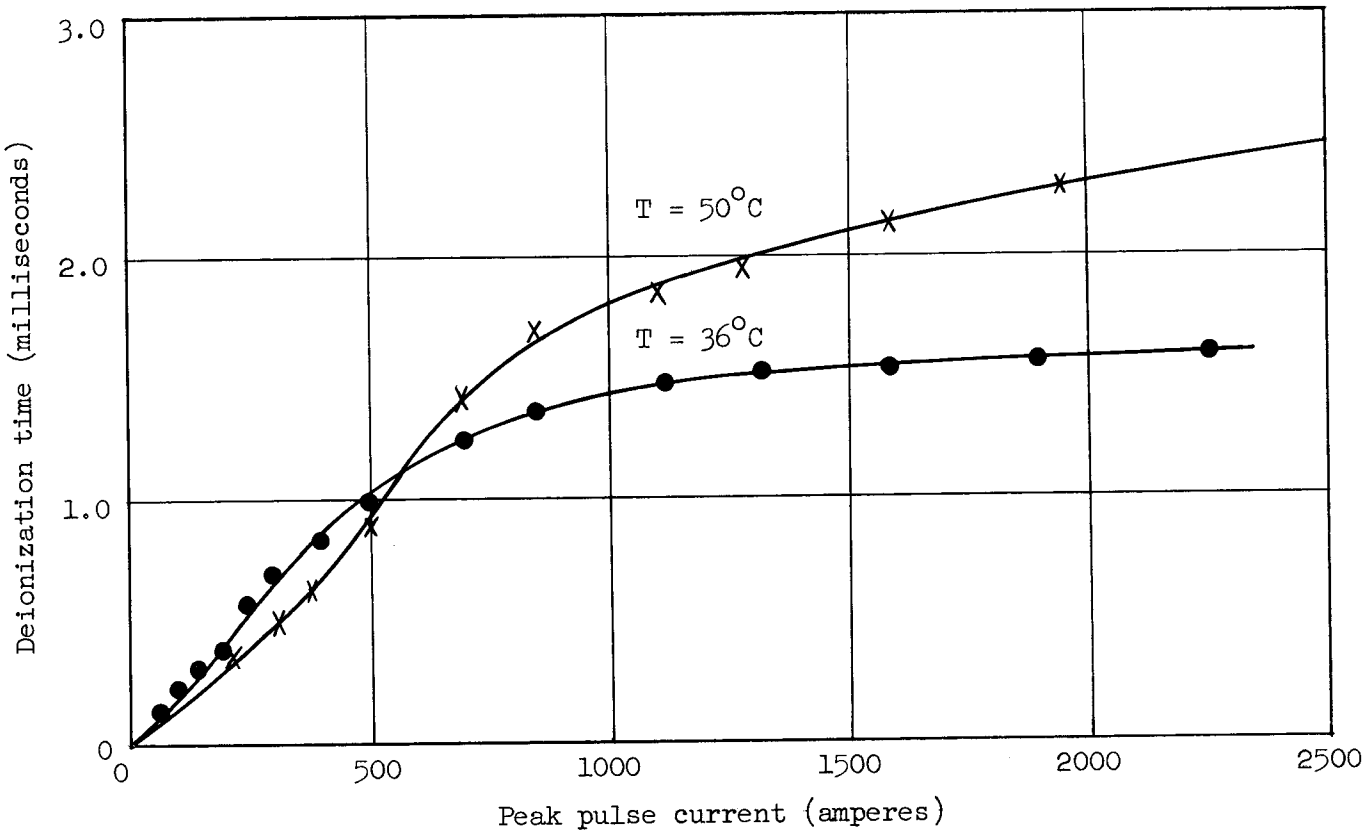

FIG. 8a--Deionization time in the cathode-shield grid region vs peak arc current for two cooling-water temperatures.

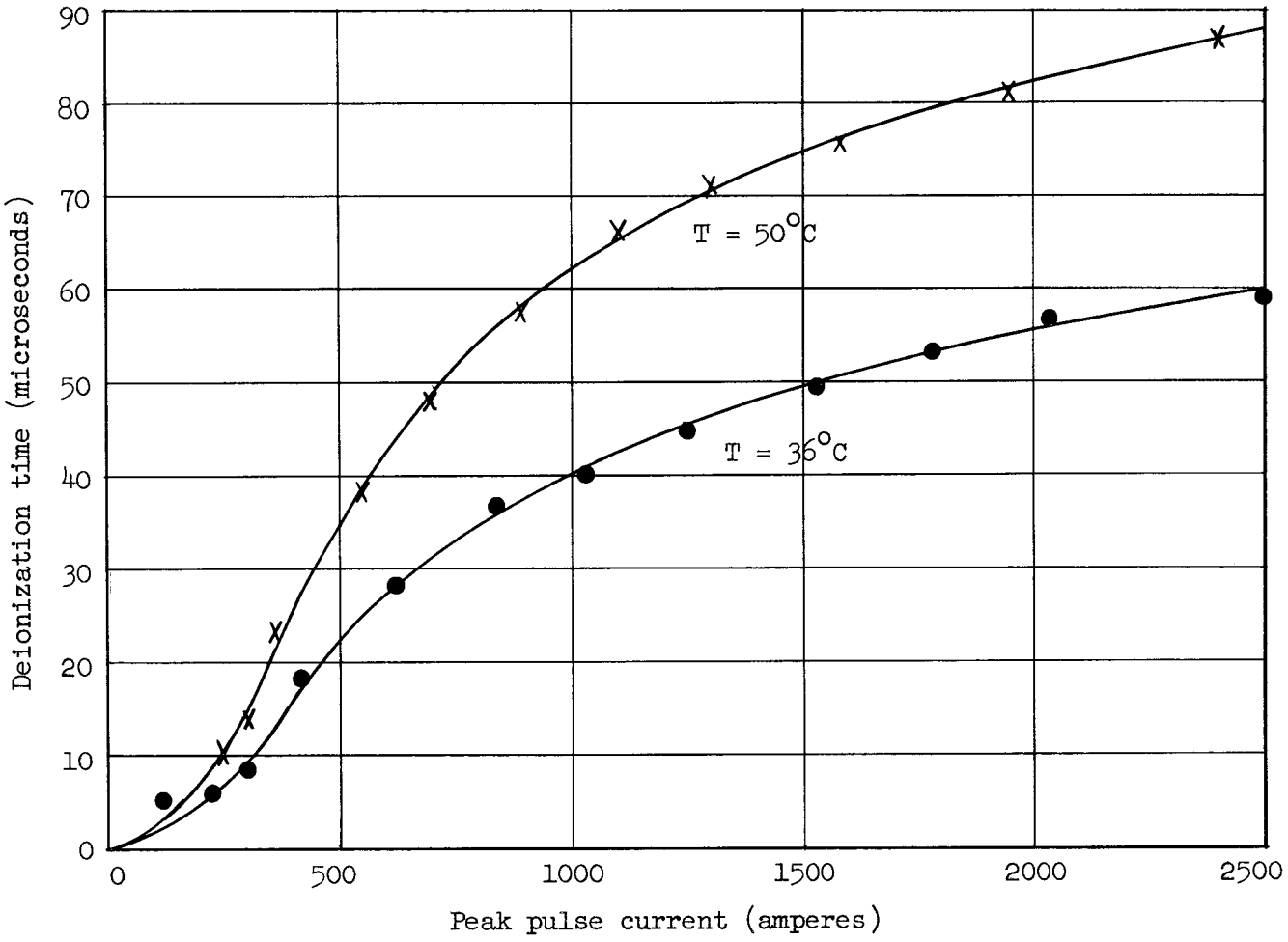

FIG. 8b--Deionization time in the control grid region vs peak arc current for two cooling-water temperatures.

both regions increased with increasing cooling water temperature. This is simply a reflection of the fact that at the higher temperature the pressure and gas density are higher and more atoms are available for point ionization. This conclusion is emphasized by Fig. 9, which shows the deionization time plotted versus cooling-water temperature for fixed arc current and fixed pulsed repetition frequency. The deionization time increases steadily with temperature. The variation of the points from the expected straight line is ascribed to experimental uncertainties.

The deionization time is also found to vary with pulse repetition frequency, as shown by Fig. 10. This is a reflection of the known fact that the mercury vapor pressure that exists in the ignitron during operation corresponds to a temperature in excess of the cooling-water temperature. With each pulse mercury is boiled off at the rate of 0.75 grams per hundred ampere seconds. The longer and more frequent the pulse, the greater the amount of mercury evaporated into the body of the tube. Some but not all of the excess condenses out. A steady state is reached in which there exists an effective vapor pressure corresponding to a temperature in excess of the temperature of the cooling-water.

3. Pulse Period

As previously noted, Figs. 8a and 8b suggest that for peak currents in excess of 2,000 amperes one is dealing with an essentially fully ionized plasma. A complete qualitative theory for the pulse period cannot be presented at this time. At higher peak currents one would expect some form of a "pinch"[10] in which the radius of the discharge column would contract due to the self-magnetic field of the current being carried by the column. Cummings[4] observed and photographed some pinches at arc currents of 10,000 amperes. However, under our operating

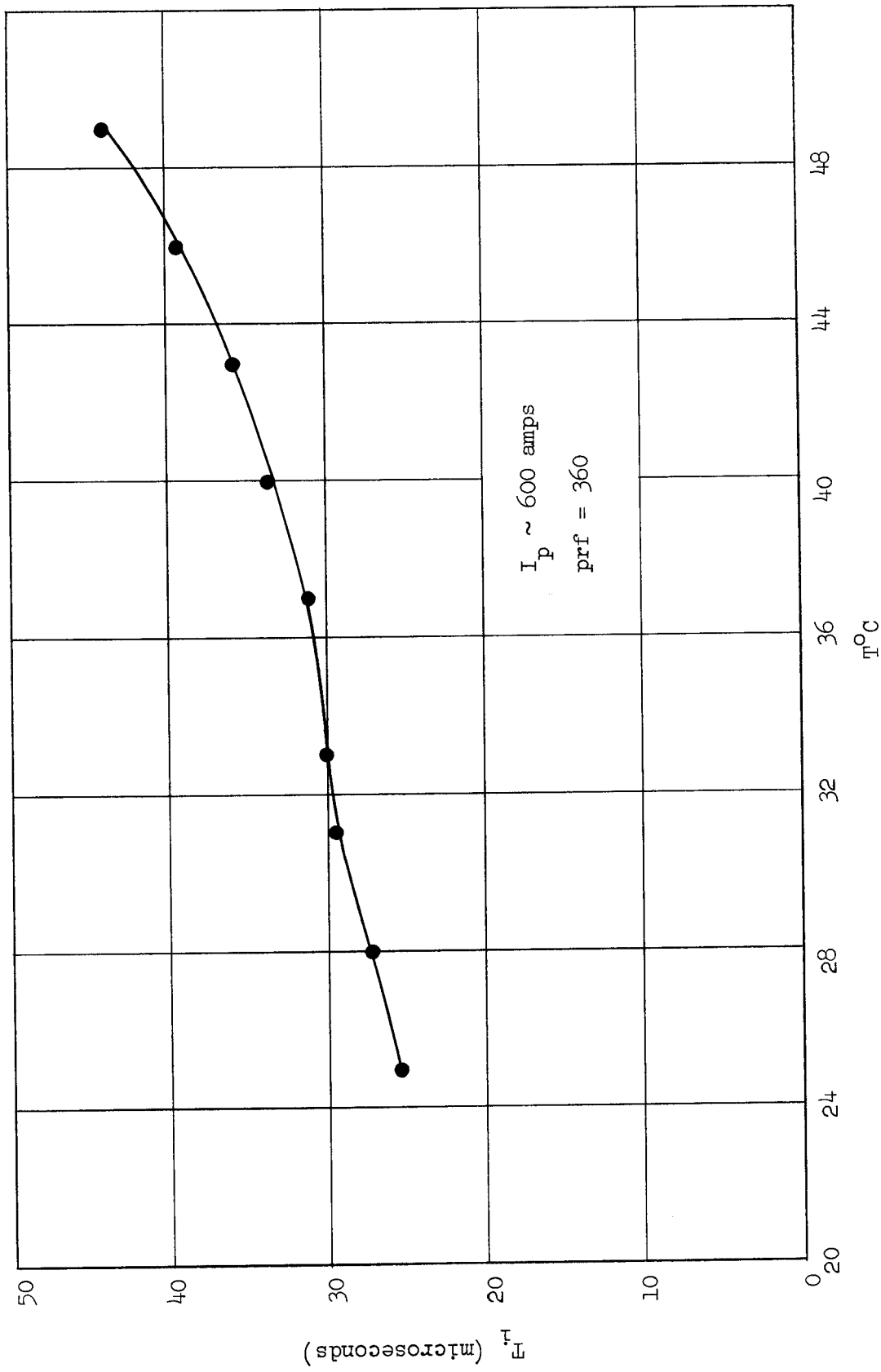

FIG. 9--Effect of cooling-water temperature on deionization time.

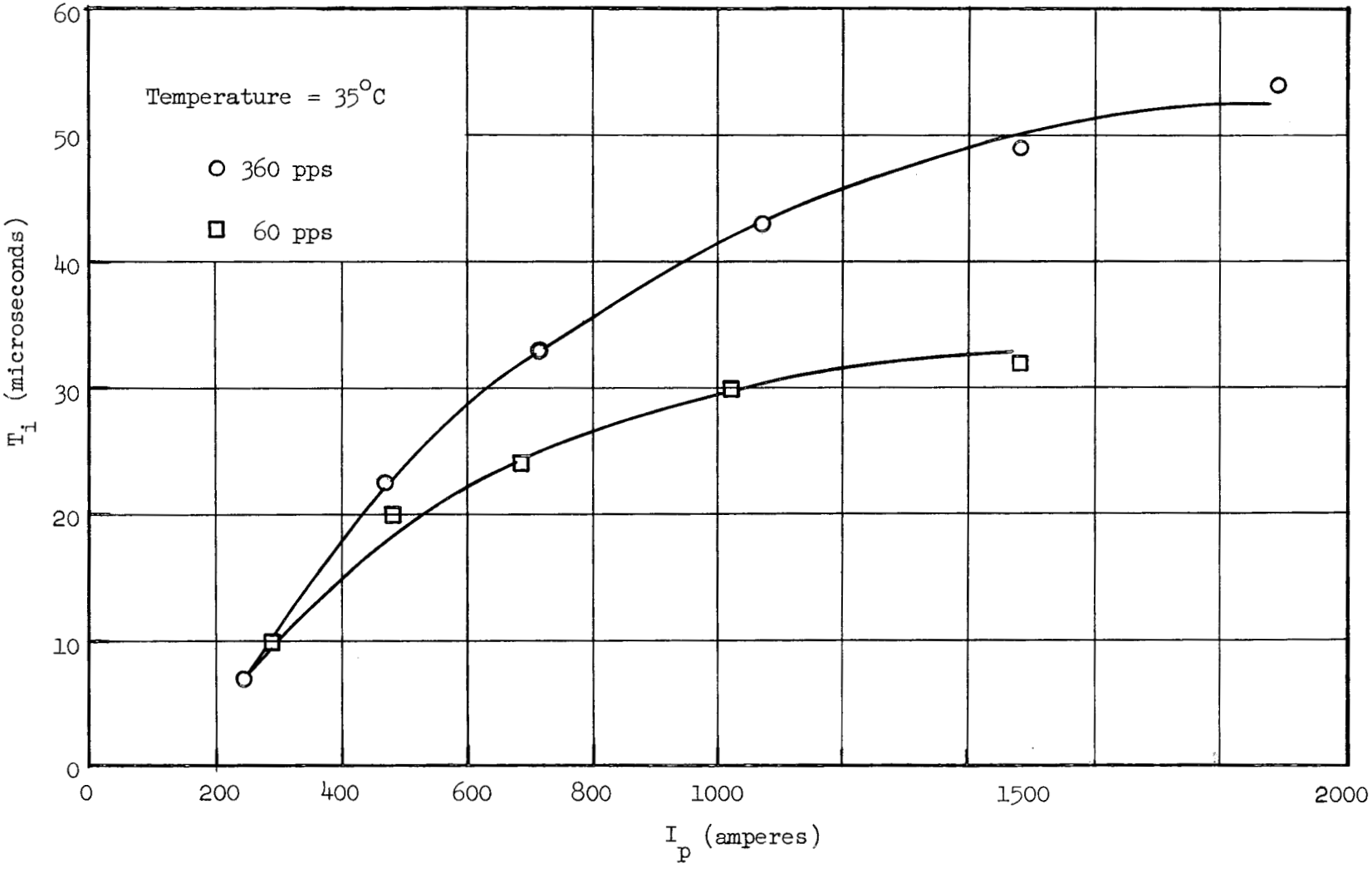

FIG. 10--Deionization time at the control grid vs peak current for two pulse repetition rates.

conditions it seems certain that the plasma is not pinching.

One interesting observation relates to an oscillation noted in the arc current pulse waveform. It was a damped oscillation with a time constant of 0.6×10^{6} sec^{-1} and a frequency of 5 Mc/sec. The amplitude was solely a function of the cooling-water temperature, increasing with increasing temperature. It was barely noticeable at $T = 36^{\circ}C$, but was quite prominent at $T = 50^{\circ}C$. This characteristic can be understood by noting that the amplitude is a function of the initial time rate of increase of arc current. At the higher cooling-water temperatures dI/dt is larger because of the higher residual ionization left in the cathode-shield grid region as a result of the increased vapor pressure and particle density. The fact that the frequency and damping factor did not change with pressure suggests that the origin of the oscillation is in the ignitron tube itself and not in the plasma column. Efforts are being made to isolate the source of this oscillation.

We conclude this section by summarizing the order of events in the ignitron, beginning at the end of the hold-off period with the tube in an essentially quiescent condition.

The ignitor fires and forms a cathode spot.

The tube is switched on. The electrons from the cathode spot are accelerated toward the anode, the arc discharge forms, and the current pulse begins. The degree of ionization and the electron and ion temperatures quickly reach their steady-state values.

When the pulse network is discharged, the tube is switched off. The plasma in the space between the grids begins to deionize. Simultaneously, the arc column expands toward the water-cooled walls of the

tube by ambipolar diffusion. There deionization of the cathode-shield grid region begins.

The external circuit recovers and begins to build up voltage for the next pulse. The inter-grid plasma decays before appreciable voltages are built up. Deionization proceeds more slowly in the cathode-shield grid space but, because this space does not have to hold off any voltage, no breakdown occurs.

The hold-off voltage reaches its maximum value. Deionization is essentially complete in the cathode-shield grid space. The tube is again ready for firing.

V. CONCLUSIONS

As the result of an extensive program of experimentation we have concluded that commercially available ignitron tubes can be used successfully as high-power switches. Specifically they make possible the development of modulators which satisfy the requirements outlined in the Introduction for the modulators in the proposed Stanford two-mile linear electron accelerator. (See Figs. 11 and 12.) However, in many ways they surpass these specifications and offer promise for providing an order of magnitude advance in high-power switch capabilities plus very long switch-tube lifetimes. They should be especially useful in boosting the power output potentials of land-based radar installations.

An additional outgrowth of our experiments was a collection of observations that contributed to our understanding of the pulsed operation of ignitrons. Based on these observations we designed an ignitron specifically for high-power switching purposes. (See Fig. 13.) Its performance is currently being evaluated.

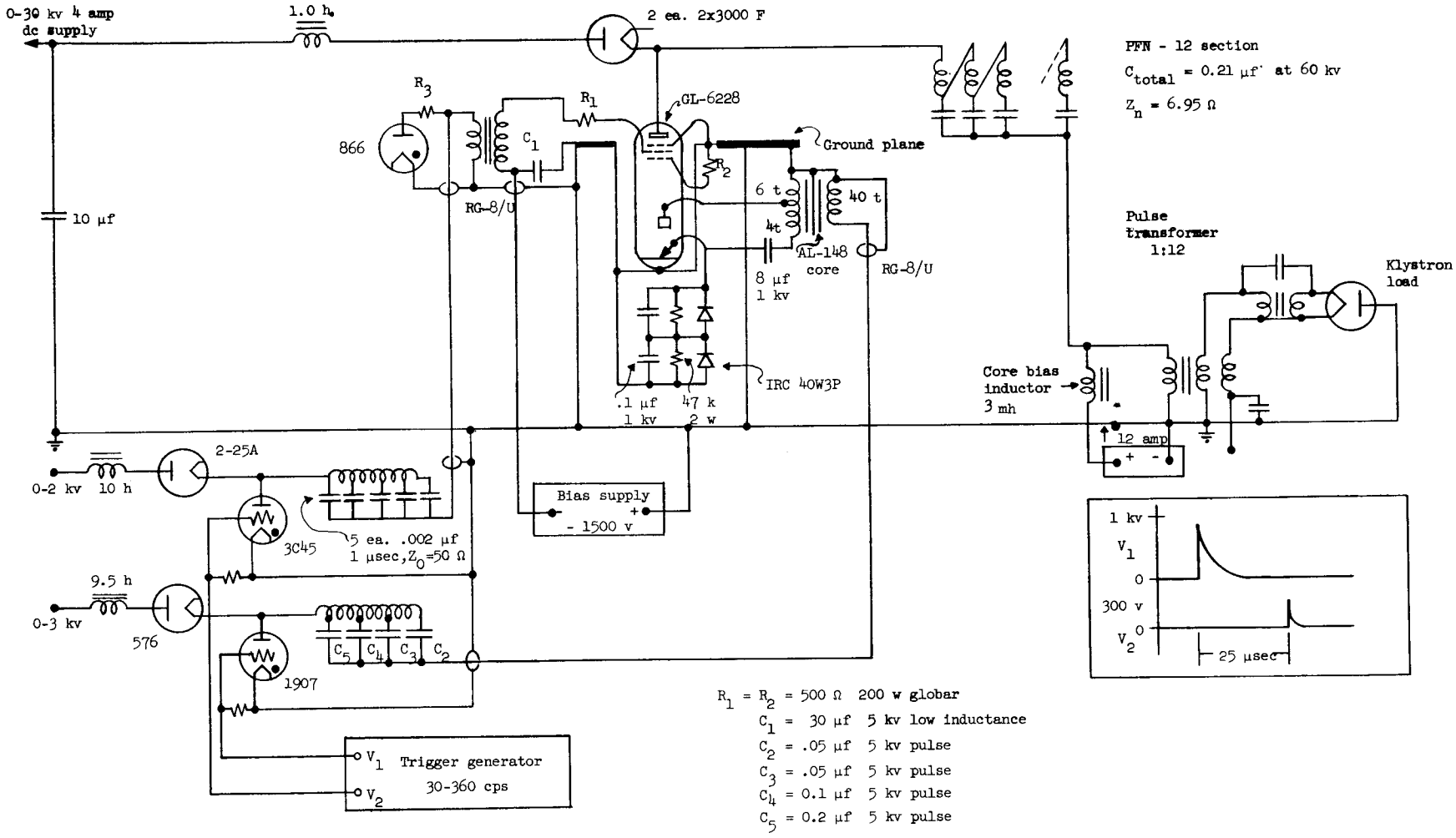

FIG. 11--Circuit diagram for 87 Mw, 110 kw modulator.

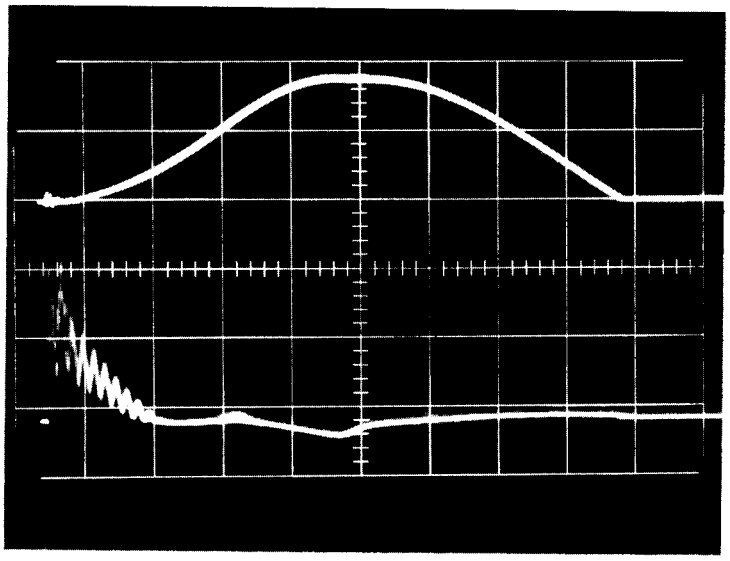

Scale: 5 μsec/cm

Fig. 12--Ignitor voltage (bottom curve) and holding anode current for GL-6228 operated in circuit of Fig. 11. The peak holding anode current is 225 amperes. The peak ignitor voltage is 400 volts. The control grid is fired at holding anode current maximum.

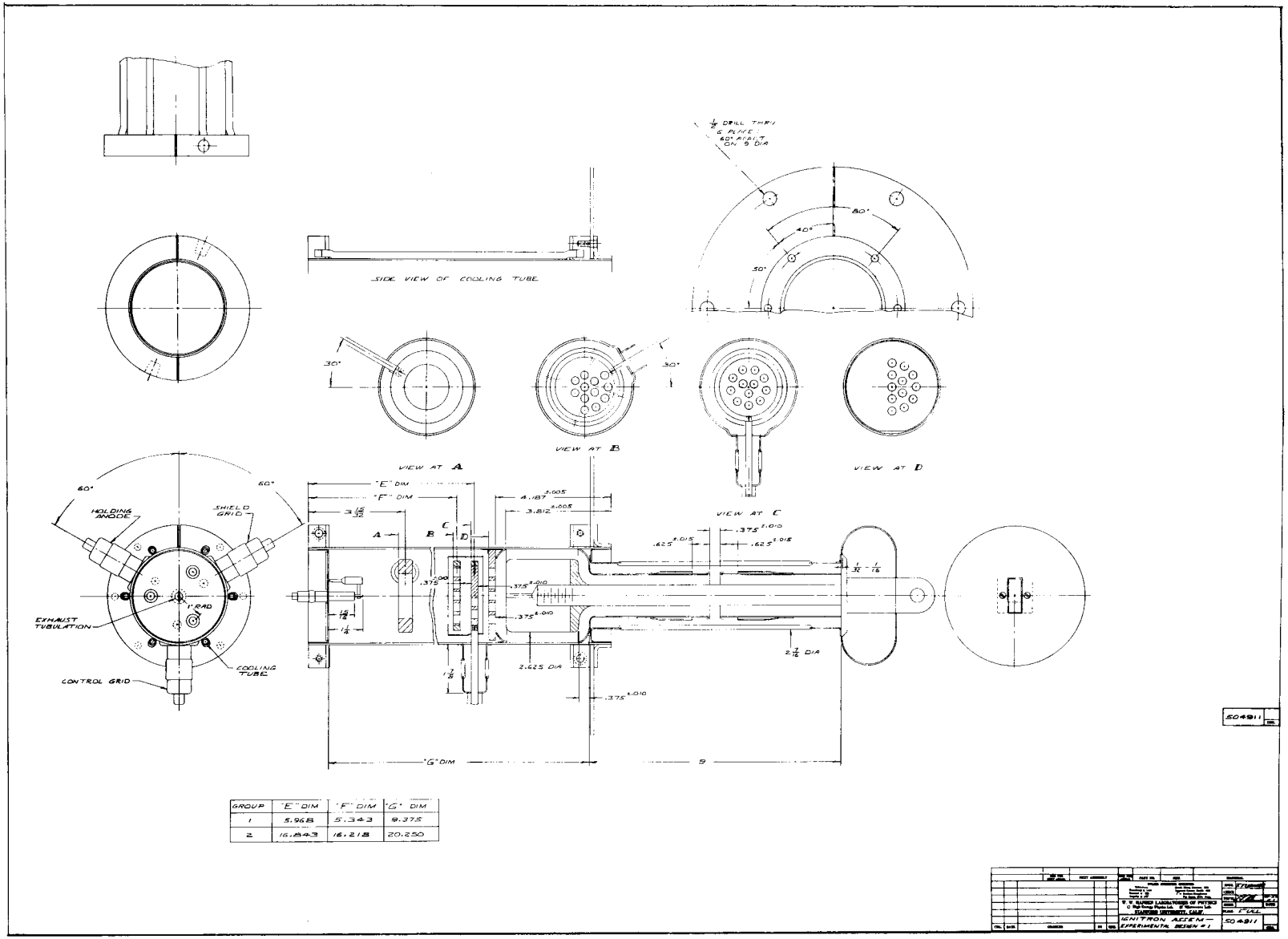

GROUP	"E" DIM	"F" DIM	"G" DIM
1	5.968	5.343	9.375
2	16.843	16.218	20.250

Fig. 13--Ignitron assembly--experimental design #1.

LIST OF REFERENCES

1. In its first phase of operation, the two-mile accelerator would produce a maximum electron energy of 20 Bev with an average beam current of 30 μamps at that energy. Radiofrequency power would be supplied by 240 klystron amplifiers, each delivering up to 24 megawatts of peak power at the design frequency of 2856 Mc/sec. Each klystron would have its own modulator. By increasing the complement of klystrons to 960, it would be possible to increase the beam energy to 40 Bev and the average beam current to 60 μamps. For a general description of the proposed Stanford machine, see R. B. Neal and W.K.H. Panofsky, "Progress Report on Proposed Stanford Two-Mile Linear Electron Accelerator," Proceedings of CERN Conference on High Energy Accelerators, CERN, Geneva, 1959.
2. H.C. Steiner, J.L. Zehner, and H.E. Zuvers, Trans. Am. Inst. Elec. Engrs., 63 (1944).
3. M. J. Mulhern, Trans. Am. Inst. Elec. Engrs., 69 (1950).
4. D. B. Cummings, UCRL Report No. 5687, Electronic Engineering Department, Radiation Laboratory, University of California, Livermore, California (June 3, 1960).
5. For an indication of the mercury ion bombardment damage possible to the ignitor structure, see D. B. Cummings, UCRL Report No. 5411, Electronic Engineering Department, Radiation Laboratory, University of California, Livermore, California (November 1958).
6. J. O. Craggs and J. M. Meek, High Voltage Laboratory Technique (Butterworth Pub. Co., London, 1954), p. 204.

7. See, for example: Internal Report No. LE 306-1, Electronic Engineering Department, Radiation Laboratory, University of California, Livermore, California (March 25, 1959).

8. Craggs and Meek, op. cit., p. 204.

9. See, for example: A. Von Engel, Ionized Gasses (Clarendon Press, Oxford, 1955) pp. 169-173.

10. This topic is discussed in almost any book on plasma physics, for example:

L. Spitzer, Physics of Fully Ionized Gasses (Interscience Publishers, Inc., New York, 1956), pp. 41-43.

A. S. Bishop, Project Sherwood (Addison-Wesley Publishing Co., Reading, Massachusetts, 1958), p. 24.

An especially clear exposition is in

S. Glasstone and R. H. Lovberg, Controlled Thermonuclear Reactions (D. Van Nostrand Co., Inc., Princeton, New Jersey, 1960), pp. 55-56.